

La_{0.7}Sr_{0.3}MnO₃ nanoparticles coated with fatty amine

Rajashree Rajagopal, J. Mona, S. N. Kale, Tanushree Bala, Renu Pasricha et al.

Citation: *Appl. Phys. Lett.* **89**, 023107 (2006); doi: 10.1063/1.2210080

View online: <http://dx.doi.org/10.1063/1.2210080>

View Table of Contents: <http://apl.aip.org/resource/1/APPLAB/v89/i2>

Published by the [AIP Publishing LLC](#).

Additional information on *Appl. Phys. Lett.*

Journal Homepage: <http://apl.aip.org/>

Journal Information: http://apl.aip.org/about/about_the_journal

Top downloads: http://apl.aip.org/features/most_downloaded

Information for Authors: <http://apl.aip.org/authors>

ADVERTISEMENT



**MATERIAL SCIENCE RESEARCH
AT 3K – MADE SIMPLE**

MONTANA INSTRUMENTS
COLD SCIENCE MADE SIMPLE

CLOSED CYCLE OPTICAL CRYOSTATS

La_{0.7}Sr_{0.3}MnO₃ nanoparticles coated with fatty amine

Rajashree Rajagopal, J. Mona, and S. N. Kale^{a)}

Department of Computer Science, Fergusson College, Pune 411 004, India

Tanushree Bala, Renu Pasricha, P. Poddar, M. Sastry,^{b)} and B. L. V. Prasad^{c)}

Materials Chemistry Division, National Chemical Laboratory, Pune 411 008, India

Darshan C. Kundaliya and S. B. Ogale^{d)}

Center for Superconductivity Research, University of Maryland, College Park, Maryland 20742

(Received 21 February 2006; accepted 21 April 2006; published online 12 July 2006)

We report on the synthesis of La_{0.7}Sr_{0.3}MnO₃ (LSMO) nanoparticles having perovskite structure and particle size of the order of 30 nm. The process involves citrate-gel synthesis, size filtering, and surface coating with a shell of octadecyl amine (ODA) using electrostatic interaction-assisted novel chemical route. Magnetic measurements show the Curie temperature of ~ 360 K establishing the desired stoichiometry and phase. Fourier transform infrared studies bring out that the amine group of ODA interacts with the LSMO surface. Refluidization yields uniform redispersion of the coated and dried powder. © 2006 American Institute of Physics. [DOI: 10.1063/1.2210080]

Colossal magnetoresistive (CMR) manganites are of considerable interest to the field of Spintronics.^{1–10} Most work on these systems has been performed on crystalline, polycrystalline and thin film forms, and hardly any efforts have been expended towards the synthesis of manganite nanoparticles to explore their use in new application areas such as biomedical diagnostics/cure and magneto-fluidics. Synthesis of stoichiometric manganite nanoparticles seems non-trivial although some useful attempts have been reported.^{8,11} For most biomedical and magnetofluidic applications one needs magnetic nanoparticles of fairly uniform size having a Curie temperature above room temperature. La_{0.7}Sr_{0.3}MnO₃ (LSMO) is a typical composition which is of interest in this context due to its high T_C of ~ 380 K and a large magnetic moment at room temperature.^{1,12–14} This system is fairly metallic and can have large microwave absorption with the possibility of its use in hyperthermia applications.¹⁵ The large moment can also allow its use in marker experiments in biodetection.¹⁵ However, in order to enhance its biocompatibility one may have to coat these particles with appropriate macromolecules. Octadecyl Amine (CH₃(CH₂)₁₇NH₂ referred as ODA) is a much used fatty amine for coating various nanoparticles.^{16,17} In this letter, we report on the synthesis and characterization of ODA-encapsulated LSMO nanoparticles.

The citrate-gel route was employed to synthesize LSMO nanoparticles. The as synthesized particles were found to be in the size range of 30–100 nm. A chemical route was then employed to isolate ~ 30 nm particles and to encapsulate them with an ODA overcoat.

Lanthanum acetate hydrate, strontium acetate hydrate, and manganese (II) acetate tetrahydrate were used as precursors in this method. Proper stoichiometric quantities of these components were dissolved in water. This solution was mixed with citric acid solution in 1:1 volume ratio. On heating this mixture in water bath at 80 °C, a yellowish transparent gel was formed on complete evaporation of water.

Continued heating caused the gel to swell and fill the beaker with a foamy precursor. Upon subjecting it to a temperature of 400 °C for 2 h, the foamy precursor decomposed to give very light, homogenous, black-colored flakes of extremely fine particle size. Further, the powder obtained by crushing these flakes was subjected to final sintering temperature of 800 °C for duration of 2 h. The powder was magnetically filtered to ensure that there are no traces of carbon in the sample. To coat these nanoparticles, the powder was mixed with equal quantity of ODA and heated to 100 °C with continuous stirring to ensure that coating is done in the paramagnetic temperature regime of LSMO. This procedure was employed specifically to avoid clustering of magnetic nanoparticles by ferromagnetic contact interactions before the ODA coating takes place and to ensure uniform coating on the entire particle surface of each particle. The mixture was continuously stirred to enable sufficient interaction between LSMO and ODA particles, resulting in a uniform dispersion of the LSMO powder in the ODA. This solution was added to chloroform and the molarity of 10⁻²M was attained. Resting this dispersion overnight gave sufficient time for the heavier LSMO particles/ agglomerates to settle to the bottom of the sealed container, whereas the lighter particles with adequate ODA coat remained in suspension. This dispersion of LSMO-ODA particles was decanted and purified using methanol. In this process of methanol-assisted precipitation, the capped particles were first separated from the solvent, and then washed twice with methanol to remove excess ODA off their surface. This purified powder was naturally dried and subjected to various characterization techniques. XRD pattern of the uncoated LSMO powder (not shown) established phase formation.¹⁰ The average particle size was estimated to be within the range of 20–100 nm using Scherrer's formula.

Figure 1 shows the FTIR spectrum of pure ODA (a), LSMO-ODA (b), and uncoated LSMO (c) powders, respectively, recorded with a KBr pellet. The peaks obtained at 3333 cm⁻¹ (feature I) and 1567 cm⁻¹ (feature II) in the case of pure ODA can be attributed to N–H stretching (NH₂ pure amine) and N–H bending vibrations, respectively. These features are completely broadened in the case of ODA-LSMO nanoparticles. A slight dip in the range of 1465–1586 cm⁻¹

^{a)}Electronic mail: snkale@pn2.vsnl.net.in

^{b)}Current address: Tata Chemicals Pvt. Ltd., Mumbai 400 059, India.

^{c)}Electronic mail: pl.bhagavatula@ncl.res.in

^{d)}Electronic mail: ogale@squid.umd.edu

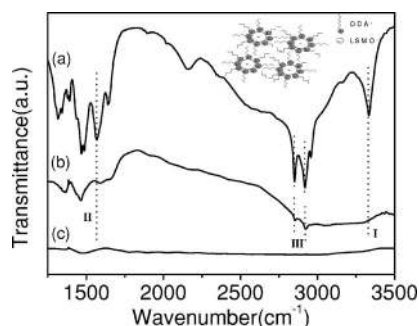


FIG. 1. Shows the FTIR spectrum of pure ODA, LSMO-ODA, and uncoated LSMO powders as shown in (a), (b), and (c), respectively, recorded with a KBr pellet. The inset shows the schematic of the type of electrostatic interaction and probable microscopic structure of the LSMO sample being encapsulated with ODA molecules.

in LSMO-ODA curve can also be attributed to the LSMO signature, as seen in Fig. 1(c). The disappearance of N–H stretching, and broadening of N–H bending vibrational groups, clearly indicates that the amine group of ODA interacts with the LSMO molecules at the surface, thereby exhibiting an electrostatic interaction, as shown schematically in the inset of Fig. 1. The features at 2920 and 2850 cm^{-1} (feature III) are due to methylene antisymmetric and symmetric vibrations, respectively, which remain common in both the cases, with the intensity ratio of the order of 1.1.

Figure 2(a) shows M - T curves of uncoated and coated LSMO nanoparticles. In both cases the Curie temperature is seen to be ~ 360 K, which brings out the good stoichiometric and phase-pure nature of the synthesized, size separated, and coated nanoparticles. It is important to mention here that in $\text{La}_{1-x}\text{Sr}_x\text{MnO}_3$, the Curie temperature is not very sensitive to composition in the proximity of the composition used by us. Hence the shape of the $M(T)$ curve cannot be regarded as a definitive proof of the right composition. We checked the

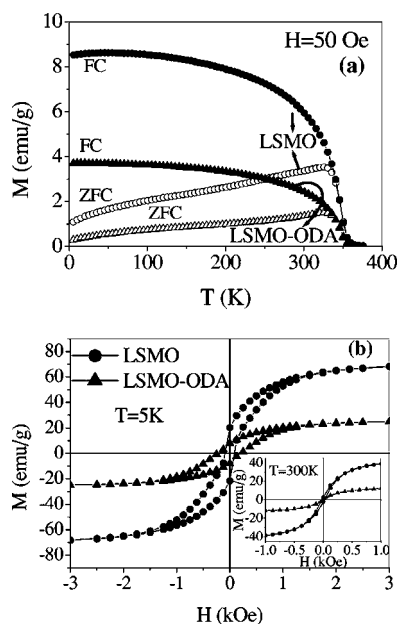


FIG. 2. (a) shows M - T curves of uncoated (circles) and coated LSMO (triangles) nanoparticles measured at 50 Oe. Filled and open symbols represent FC and ZFC, respectively. The transition temperature is seen to be 370 K in both the cases. (b) shows hysteresis curves for both the samples taken at 5 K. The inset shows magnetization isotherms taken at room temperature. The low temperature moment of ODA coated LSMO was seen to be 25 emu/g and of uncoated sample as 70 emu/g .

mean composition of the pressed compacts made from the powders by two techniques, namely scanning electron microscopy with wavelength dispersive spectroscopic x-ray analysis (WDS) and Rutherford Backscattering (RBS), both data calibrated against high temperature sintered pellet and scanned at different points. The composition was uniform and close to the intended one ($\text{La}_{0.7}\text{Sr}_{0.3}\text{MnO}_3$) to within $\sim 5\%$. To obtain the composition of each nanoparticle and see particle-to-particle variation one would have to perform high resolution scanning TEM with electron energy loss spectroscopy (EELS) which is a highly specialized tool not easily accessible.

Figure 2(b) shows the hysteresis loops for both the samples taken at 5 K and at room temperature. The curves for both the samples show saturation magnetization at around 2500 Oe. The coercivities at 5 K were found to be 250 Oe for the uncoated sample and 500 Oe for ODA coated LSMO. The larger coercive field of the ODA coated system reflects interparticle isolation due to the coat and the single domain character of the individual nanoparticles. As is known large multidomain particles of LSMO have much lower coercive field of 100 Oe or less. The lower coercive field of the uncoated particles as compared to the coated ones reflects collective domains in the uncoated system due to magnetic contact and proximity. Interestingly, as seen in Fig. 2(a), the saturation moment of ODA coated sample in terms of emu/g is seen to be substantially lower than the uncoated one. The moments observed in our uncoated nanoparticles (~ 73 emu/g at 5 K and ~ 45 emu/g at 300 K) are completely consistent with (and, in fact, higher than) the reported values.^{18,19} Given the identical Curie temperature and other similar LSMO characteristics for both the uncoated and coated samples, the lower emu/g for the coated system may *a priori* reflect the extra weight of ODA per particle. However, as we show below the large magnitude of drop is quantitatively not consistent with the weight estimate of ODA coat suggesting a more basic influence of ODA coating on nanoparticle magnetization.

Figure 3(a) shows the TEM micrograph of ODA coated and size separated nanoparticles. This clearly shows the agglomerate of $\sim 30 \pm 5$ nm nanoparticles with clear interparticle separation. Since the ODA coating process was deliberately implemented at a temperature above the Curie temperature of LSMO by heating, the origin of the observed agglomeration may be in the van der Waals forces or chemical forces between the protruding molecular chains during the final drying stages. The magnetic interaction between coated particles, which is essentially dipolar one with macromolecular separation, cannot be strong enough to cause magnetic agglomeration. However, rapid cooling below Curie temperature during fluidization may also contribute to some degree of agglomeration on contact. These issues remain to be resolved by further work. It is gratifying, however, that the particles obtained by our process clearly have a separating ODA coat as we further establish by refluidization experiment discussed below. A very recent communication²⁰ reveals that clustering of magnetic nanoparticles (Fe_3O_4) can be stabilized and hence controlled by using a polymer coat.

In Fig. 3(b) we show the result of thermogravimetric analysis (TGA) on the ODA coated size separated LSMO nanoparticles. The loss of weight upon ODA evaporation expected to be completed by 400 $^\circ\text{C}$ is about 4%–5%. Given the fact that the ODA loading of nanoparticle weight is only

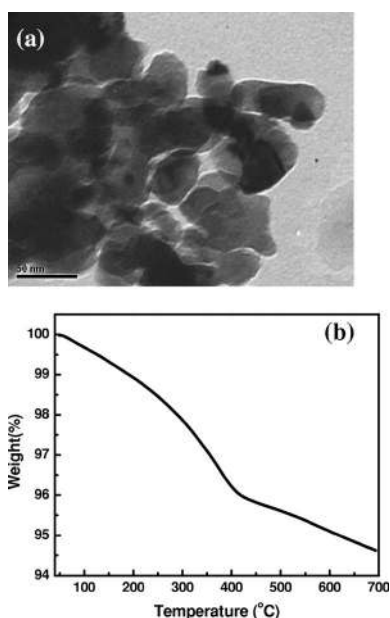


FIG. 3. Shows representative AFM image of a drop-coated LSMO-ODA nanoparticle assembly. The low magnification image clearly reveals the organization of grains with the grain size of the order of 300 nm. The inset shows TEM micrograph of one grain. Assembly of ~ 30 nm nanoparticles in the form of bigger grains and a coat of ODA is also clearly seen in the micrograph.

about 4%–6%, the observed large drop^{21–23} in magnetic moment (emu/g) has to be explained by other mechanisms, such as the charge transfer across the adsorption interface and the influence of attendant electric field effects on manganite,^{22,24} the sensitivity of manganite properties to various factors,²⁵ interparticle interactions, etc.

Finally, in Fig. 4 we show (a) the original decanted solution showing uniform suspension of ODA coated particles, (b) methanol-assisted precipitation through two washing cycles before drying the powder, and (c) and (d) refluidization of the ODA coated dry powder in chloroform at two different concentrations showing fully uniform dispersion once again. This demonstration shows that the coating process demonstrated here renders uniform coating capable of uniform re-dispersion.

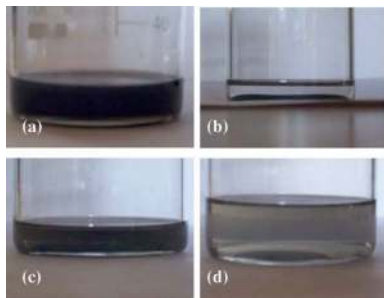


FIG. 4. (a) shows the decanted solution prior to purification, showing uniform suspension of ODA coated LSMO particles. (b) shows the particles precipitated out of methanol after two washing cycles. (c) and (d) show the results after refluidization in chloroform of the dry ODA coated powder at two different concentrations, namely, 0.1 and 0.05 mg/ml, respectively, clearly indicating fully uniform dispersion once again.

In conclusion, we have synthesized, size separated, and characterized ODA coated nanoparticles of mixed-valent manganite LSMO. The particles exhibit a Curie temperature of ~ 360 K, close to stoichiometric phase-pure LSMO. FTIR spectra show that the amine group of ODA interacts with the surface of LSMO. Refluidization experiment ensures uniform coating on particles enabling redispersion.

The authors at Fergusson College would like to thank UoP-ISRO interaction cell (PU/DESPUN/2005/1/III), Professor C. V. Dharmadhikari (Pune University) and Dr. Alok Bokare of Agharkar Research Institute. Two of the authors (S.B.O. and D.C.K.) acknowledge support under NSF-MRSEC Grant No. DMR-0520471.

¹H. Y. Huang, S. W. Cheong, N. P. Ong, and B. Batlogg, *Phys. Rev. Lett.* **77**, 2041 (1996).

²K. Ghosh, S. B. Ogale, R. Ramesh, R. L. Greene, T. Venkatesan, K. M. Gupchup, Ravi Bathe, and S. I. Patil, *Phys. Rev. B* **59**, 533 (1999).

³H. L. Ju, J. Gopalakrishnan, J. L. Peng, Qi Li, G. C. Xiong, T. Venkatesan, and R. L. Greene, *Phys. Rev. B* **51**, 6143 (1995).

⁴J. Heremans, *J. Phys. D* **26**, 1149 (1993).

⁵C. N. R. Rao and B. Raveau, *Colossal Magnetoresistance, Charge Ordering and Related Properties of Manganese Oxides* (World Scientific, Singapore, 1998).

⁶K. I. Kobayashi, T. Kimura, H. Sawada, K. Terakura, and Y. Tokura, *Nature (London)* **395**, 677 (1998).

⁷S. L. Yuan, G. Q. Zhang, G. Peng, F. Tu, X. Y. Zeng, J. Liu, Y. P. Yang, Y. Jiang, and C. Q. Tang, *J. Phys.: Condens. Matter* **13**, 5691 (2001).

⁸Jeffrey J. Urban, Lian Ouyang, Moon-Ho Jo, Dina S. Wang, and Hongkun Park, *Nano Lett.* **4**, 1547 (2004).

⁹J. Rivas, L. E. Hueso, A. Fondado, F. Rivadulla, and M. A. Lopez-Quintela, *J. Magn. Magn. Mater.* **221**, 57 (2000).

¹⁰A. de Andres, M. Garcia-Hernandez, J. L. Martinez, and C. Prieto, *Appl. Phys. Lett.* **74**, 3884 (1999).

¹¹Carlos Vazquez-Vazquez, M. Carmen Blanco, M. Arturo Lopez-Quintela, Rodolfo D. Sanchez, Jose Rivas, and Saul B. Oseroff, *J. Mater. Chem.* **8**, 991 (1998).

¹²A. Chainani, M. Mathew, and D. D. Sarma, *Phys. Rev. B* **47**, 15397 (1993).

¹³Z. Trajanovic, C. Kwon, M. C. Robson, K. C. Kim, M. Rajaswari, S. E. Lofland, S. M. Bhagat, and D. Fork, *Appl. Phys. Lett.* **69**, 1005 (1996).

¹⁴H. Asano, S. B. Ogale, J. Garrison, A. Orozoco, Y. H. Li, V. Smolyaninova, C. Gally, M. Downes, M. Rajeshwari, R. Ramesh, and T. Venkatesan, *Appl. Phys. Lett.* **74**, 3696 (1999).

¹⁵Q. A. Pankhurst, J. Connolly, S. K. Jones, and J. Dobson, *J. Phys. D* **36**, R167 (2000).

¹⁶Anand Gole, Chandranu Dash, Mala Rao, and Murali Sastry, *Chem. Commun. (Cambridge)* **4**, 297 (2000).

¹⁷A. Swami, P. R. Selvakannan, R. Pasricha, and M. Sastry, *J. Phys. Chem. B* **108**, 19269 (2004).

¹⁸L. Balcells, B. Martinez, F. Sandiumenge, and J. Fontcuberta, *J. Phys.: Condens. Matter* **12**, 3013 (2000).

¹⁹Y. W. Duan, X. L. Kou, and J. G. Li, *Physica B* **355**, 250 (2005).

²⁰Andre Ditsch, Paul E. Laibinis, Daniel I. C. Wang, and T. Alan Hatton, *Langmuir* **21**, 6006 (2005).

²¹J. Hormes, H. Modrow, H. Bonemann, and C. S. S. R. Kumar, *J. Appl. Phys.* **97**, 10R102 (2005).

²²M. Aslam, L. Fu, S. Li, and V. P. Dravid, *J. Colloid Interface Sci.* **290**, 444 (2005).

²³S. Cho, B. R. Jarrett, A. Y. Louie, and S. M. Kauzlarich, *Nanotechnology* **17**, 640 (2006).

²⁴T. Wu, S. B. Ogale, J. E. Garrison, B. Nagaraj, A. Biswas, Z. Chen, R. L. Greene, R. Ramesh, T. Venkatesan, and A. J. Millis, *Phys. Rev. Lett.* **86**, 5998 (2001), see also S. B. Ogale, V. Talyansky, C. H. Chen, R. Ramesh, R. L. Greene, and T. Venkatesan, *ibid.* **77**, 1159 (1996).

²⁵M. B. Salamon and M. Jaime, *Rev. Mod. Phys.* **73**, 583 (2001).